2021-12

Emergent coastal behaviour results in extreme dune erosion decoupled from hydrodynamic forcing

Hird, S

10.1016/j.margeo.2021.106667
Marine Geology
Elsevier BV

Emergent coastal behaviour results in extreme dune erosion decoupled from hydrodynamic forcing

Simon Hird [a] *, Christopher Stokes [a], Gerd Masselink [a]

[a] Coastal Processes Research Group, School of Biological and Marine Sciences, University of Plymouth, Plymouth, PL4 8AA, UK.

* Correspondence: simonhird1@gmail.com; Tel.: +447909885835.

Highlights

- Extreme dune erosion appears decoupled with hydrodynamic forcing
- River avulsion has resulted in beach lowering
- XBeach modelling shows beach lowering has increased vulnerability of dunes to wave action

Abstract

Coastal dune systems provide vital natural barriers against storm impacts and coastal inundation. In times of rising sea levels and uncertainty over increasing storminess, it is critical that dune erosion is adequately understood and actively monitored. This study investigates the severe erosion of the climbing dune system at Crantock, an exposed macro-tidal beach in north Cornwall, UK, that before 2013 showed relative stability. In contrast to regional consistency in beach recovery across north Cornwall since the major storms of 2013/14, Crantock beach and dune system have shown an acceleration in erosion. This has resulted in dramatic cut-back of the front of the climbing dune system since 2016, despite the reduced frequency of severe storm events since 2013/14. The decoupled nature and emergent response of Crantock's dune system are explained by the shifting channel of the River Gannel, which has its outflow over the beach. Intertidal bar movement during the recovery from the 2013/14 storm sequence, alongside an ongoing deterioration of the training wall that pinned the River Gannel to the East Pentire cliffs to the north of the beach, has led to a southward avulsion of the river that has since lowered the elevation of the beach in front of the dunes. XBeach modelling suggests that the increased dune erosion can be attributed to a lowering of the beach profile and steepening of the

dune face, indicating that the river avulsion has triggered a step-change in the dune equilibrium and the onset of dramatic erosional events.

Keywords

Dune erosion; Beach lowering; Emergent behaviour; Storm response, Storm recovery, XBeach

Funding

This research was funded by the U.K. Natural Environment Research Council, Grant Number NE/M004996/1; BLUE-coast project.

1. Introduction

Coastal dune systems have long been acknowledged to play a critical protective role against coastal inundation, acting as natural barriers for coastal communities during large wave and/or storm surge events (Bruun, 1962; Carter, 2013; Edelman, 1969). As a result, the last 50 years have seen a wealth of investigation into the drivers of dune erosion to inform more effective management of these vital natural structures (Carter and Stone, 1989; Doyle et al., 2019; Edelman, 1969; Houser et al., 2008; Pye and Neal, 1994; Splinter and Palmsten, 2012; Tătui et al., 2014; van Thiel de Vries et al., 2008; Vellinga, 1982). Against the backdrop of rising sea levels (Church et al., 2013), as well as uncertainty over increasing storminess (Castelle et al., 2018; Palmer et al., 2018), it is critical to monitor and understand coastal dune evolution and maintain the valuable natural capital they represent (Everard et al., 2010). Coastal dunes, defined as accumulations of unconsolidated sand that form in the backshore as a result of aeolian deposition (Hesp, 2005; Nordstrom and Jackson, 2012), are of particular importance as they can act as a first line of defence for coastal flooding. The development and resulting morphodynamics of coastal dunes are controlled by several parameters, including sand supply, vegetation cover, aeolian transport, wave processes, storm erosion (scarping and overwash), sea level and the extent of human impact (Hesp, 2005). Wave erosion can drive high magnitude responses in coastal dune systems, with dune retreat >10 m recorded during a single winter season (Castelle et al., 2015; Scott et al., 2016).

Coastal erosion of dunes typically only occurs at high water levels with large wave heights and setup. Wetting of the dune toe and undercutting through wave action can trigger slope failures or avalanches that result in large erosion volumes over short timescales (Carter and Stone, 1989). Clustering of storm events can lead to a disproportional morphological response by lowering bed levels, preventing interim recovery, and increasing vulnerability of dune systems to erosion from subsequent storm events (Dissanayake et al., 2015).

In contrast, aeolian processes operate over much more gradual timeframes, resulting in more subtle vertical changes on the order of 0.1 m yr^{-1} of erosion or accretion. Sand deposition and erosion on dunes is highly dependent upon wind velocities, vegetation coverage, moisture content, surface roughness and topography (Hesp, 2005). In low wind speeds (but above the critical threshold), deposition is primarily focused on the stoss side of dune face (particularly if well-vegetated) (Hesp, 2005) or dune toe, and can result in the formation of a ramp which acts to protect the dune from wave run-up processes and dune scarping (Guisado-Pintado and Jackson, 2019). Where vegetation coverage reduces, or wind speeds increase, sediment is transported further up the stoss face and can result in deposition on the dune crest (resulting in a vertical building of the dune) or in the lee (Arens, 1997; Hesp, 2005). The relative dominance between aeolian and wave processes acting upon dunes is highly variable through time, with aeolian transport and building of the dune linked to the ability of the beach face to dry out (Jackson and Nordstrom, 1997). Wave and wind erosion can both be correlated with storm events; however, aeolian erosion is typically much lower than wave erosion (Arens, 1997; Guisado-Pintado and Jackson, 2019; Hesp, 2005).

The winter of 2013/14 saw an unprecedented sequence of large, storm-induced wave events that impacted western European coastlines, driven by an unusually strong jet stream and intense polar vortex (Davies, 2015). It was reported that the 8-week period from mid-December 2013 through to mid-February 2014 was the most energetic wave period recorded on the southwest (SW) coast of England since at least 1953 (Masselink et al., 2015), and along the Atlantic coast of Europe since at least 1948 (Masselink et al., 2016). The sequence of 22 storms resulted in extensive morphological impact along

the Atlantic Coast of Europe, with many regularly monitored sites in their most eroded state since the inception of morphological records (Masselink et al., 2016; Scott et al., 2016). Highly exposed beaches such as Perranporth, (north Cornwall, UK) and Truc Vert (Gironde, France) saw sediment losses in excess of 200 m^3m^{-1} from their beach and dune systems (Masselink et al., 2016), whilst Vougot (Brittany, France) saw a retreat of its coastal dune by > 5 m (Suanez et al., 2015). Varying styles and magnitudes of morphological response were recorded, linked to large scale variability in the hydrodynamic forcing (waves heights, tides, storm surges), as well as more local factors such as geology, beach type, embayment size and angle of storm wave approach (Burvingt et al., 2017). Across the SW of England, a degree of regional coherence in morphological impact was recorded, with four main classifications of beach response identified (Burvingt et al., 2017). Along the north coast of Cornwall, findings illustrate that exposed and cross-shore transport-dominated beaches exhibited synchronous changes in beach volumes over event to multi-annual timescales (Burvingt et al., 2018). Over this 100-km stretch of coast, cross-shore dominated beaches showed coherent behaviours that were coupled in timing with hydrodynamic forcing despite variations in local characteristics such as beach size, sedimentology and degree of embayment (Burvingt et al., 2018). Whilst magnitudes were variable, the coherence of the response has been noted for its critical importance for regional management.

Practically all beaches along the north Cornish coast exhibited significant dune erosion during the 2013/14 winter, followed by relative dune stability. (Burvingt et al., 2017). However, the dune system at Crantock, deviated from this and has seen an acceleration in erosion in recent years (Konstantinou et al., 2021), with its dune system becoming dangerously steep through scarping, raising public concern (BBC, 2018; Express, 2019). The onset of the acceleration in erosion appears to coincide with the migration of the River Gannel's channel, which has its outflow across the beach. Previous investigations at Crantock have been medium- to long-term, utilising historical spatial datasets from the Ordnance Survey mapping archive (Oyedotun, 2014, 2015). Using Digital Shoreline Analysis System (DSAS), historical shoreline data were compared from five time periods, starting from 1888 up until 2012. Results indicated that Crantock showed an overall landward retreat. The mean high water (MHW)

111 contour showed a mean annual rate of change ranging from +0.26 (advance) to 1.00 (retreat) m yr^{-1},
112 whilst the mean low water (MLW) contour showed a retreat of 0.25–1.00 m yr^{-1} along the beach
113 (Oyedotun, 2014). The retreating MLW and advancing MHW resulted in a steepening of the foreshore
114 produced by a narrowing of the beach width from approximately 300-400 m in 1888 to 150 m in 2012
115 (Oyedotun, 2015). However, the datasets used had spatial accuracies of ±10 m and sampling frequencies
116 of 16–76 years, meaning both the spatial and temporal resolution of the study is low, providing only a
117 coarse understanding of coastal changes. UK coastal management strategies outline that where
118 accommodation space, high wind energy and a healthy sediment budget exists, frontal dunes should be
119 allowed to naturally roll-back to establish a new equilibrium following storm events, which is the
120 current approach adopted at Crantock (Pye, 2007). In instances where chronic dune erosion is recorded,
121 nourishment and dune protection or restoration are recommended (Pye, 2007). In order to inform the
122 effective management of Crantock dune system, it is integral to quantify the rates of dune erosion and
123 roll-back, as well as understand the reasons for the dune dynamics.
124
125 Contemporary geomorphology has seen a critique of traditional reductionist approaches to geomorphic
126 enquiry with emphasis placed upon new concepts such as complexity, emergence and contingency
127 (Murray et al., 2009). The term 'Complex' is applied to describe a system whose properties are not fully
128 explained by an understanding of its component parts (Gallagher and Appenzeller, 1999), moving
129 beyond the simple perception of linear cause and effect (Murray et al., 2014). Reductionist
130 methodologies tend to allude to the fact that a landscape is simply the sum of all the process on-going
131 in the system, but it is increasingly becoming clear that landscapes are complex non-linear systems,
132 particularly when examined from the macro-scale (Harrison, 2001). A complex system produces
133 disproportionate responses to disturbances due to an array of non-linear processes and feedback loops,
134 which can result in emergent outcomes (Favis-Mortlock, 2013). Emergent behaviour in geomorphology
135 is the formation of a whole-system output that is often surprising, as a result of the interactions from
136 many within-system processes (Favis-Mortlock, 2013; Phillips, 2011, 2014). Here, these concepts are
137 applied to the Crantock beach and dune system, where an apparent acceleration in dune erosion, in the

absence of an evident shift in hydrodynamic forcing, seems to be linked to a switch in river channel position.

The principal aim of this study is to investigate the reasons behind the accelerated dune erosion observed at Crantock several years after the extreme 2013/14 winter. The two hypotheses presented are that: (1) the acceleration is a result of the environmental forcing; or (2) it is an outcome of the sudden shift in river channel position. The objectives of the study are to: (i) quantify dune retreat and place it within a temporal framework of morphological change observed at Crantock; (ii) relate the timescale of dune retreat to boundary conditions including hydrodynamic forcing and river channel evolution; and (iii) conduct numerical modelling to investigate the sensitivity of dune retreat to the presence of the river channel on the beach face.

2. Methodology

2.1. Study site

Crantock beach is located in southwest England on the north coast of Cornwall (Figure 1a). The embayment is lined by the east and west Pentire headlands, with the latter providing a degree of shelter from the prevailing westerly wave climate from the north Atlantic. The sheltering results in a strong gradient in wave heights across the embayment, with larger waves breaking to the north, driving a clockwise current circulation resulting in a headland rip to the south of the beach. Crantock features low tide bar/rip morphology and a mean spring tidal range of 6.3 m (Buscombe and Scott, 2008; Scott et al., 2011). The River Gannel estuary flows onto the beach at the northwest corner. The channel was previously pinned to the East Pentire cliffs by a training wall, which has gradually degraded through time, and now permits the channel to meander laterally across the beach. Crantock beach is backed by an extensive grassy dune system (> 20 metres high) that has experienced extreme erosion in recent years, see Figure 1b.

The dunes at Crantock are best described as climbing dunes, which are common in Cornwall and occur '*wherever there is higher ground adjacent to a dune system and sufficient wind energy to drive the sand up the slope*' (Radley, 1994, p.28). Climbing dunes are often found in close association with cliff-top dunes and have been used extensively in Quaternary paleo-environmental reconstructions (e.g., Ho et al., 2017). Their morphodynamic behaviour is expected to be somewhat different from that of foredune systems; specifically, the fact that they are underlain by impermeable bedrock and water may flow along the interface of the dune and bedrock under extreme rainfall conditions to the detriment of the dunes. Additionally, the presence of a dune ramp (Christiansen and Davidson-Arnott, 2004), bridging the 'gap' between beach and dune sand overlying the bedrock, is essential for allowing sand to be blown from the beach into the climbing dune area. However, the dune erosional processes described in this paper are mostly the result of undercutting and sediment removal of the dunes by waves.

2.2. Environmental data

2.2.1. Wave, tide and wind data

Wave data were acquired from a Datawell Directional Waverider Mk III wave buoy, deployed at Perranporth by the Southwest Regional Coastal Monitoring Programme on 18th December 2008 (PCO, 2019b). Wave data are collected at approximately 14 m depth at mid tide. Meteorological data are also measured at Perranporth using a Vaisala WXT520 automatic weather station (1st August 2011 – present) providing wind speed and direction as well as other parameters not used here. Tide data were acquired from the Etrometa step gauge at Port Isaac, where measurements began on 15th July 2010. All wave, tide and wind data were accessed freely via the Plymouth Coastal Observatory (PCO) data portal (https://southwest.coastalmonitoring.org/).

2.2.2. River Gannel

The planform change of the river Gannel was tracked using Light Detection and Ranging (LiDAR), unmanned aerial vehicle (UAV) surveys, and aerial photography. The channel position was digitised in ArcMap 10.6 for each time step. The channel has been highly dynamic since the avulsion from its

191 former route on both seasonal and event scale timeframes, meaning that the data presented here provides
192 only a coarse picture of the channel migration. Daily mean discharge data from the River Gannel were
193 downloaded from the Environment Agency's Hydrology API (EA, 2019). Discharge is measured at the
194 Gwills monitoring station, a crump profile weir located 2 km upstream from the Gannel estuary (NRFA,
195 2019) that has been operational since 1969.
196
197 ## 2.3. Morphological survey data
198 Three types of morphological survey data with varying repeat frequencies have been utilised here, see
199 Table 1. LiDAR, supplemented with UAV data, has been used to provide an overall picture of the
200 geomorphic change observed at Crantock Beach from 2008 to 2019. Topographic profile data from
201 three cross-shore survey lines that extend from the dunes to spring low water (Figure 1a) have been
202 used to provide a finer temporal resolution dataset. Gaps in the topographic profile time series were
203 supplemented by extracting profiles from LiDAR and UAV surveys to produce a quasi-annual time
204 series. All surveys were conducted at, or close to, mean low water springs (MLWS).
205
206 ### *2.3.1. Topographic profiles and LiDAR*
207 Three profile lines are repeatedly sampled across Crantock Beach by PCO (7a01643, 7a01639 and
208 7a01634), shown in Figure 1a. Data are collected quasi-annually along each of the profiles, with
209 sampling times primarily dictated by the occurrence of significant storm events. Not all the profiles
210 have complete temporal coverage, as shown in Table 1. Profile 7a01643 was surveyed each year, whilst
211 7a01639 is missing three surveys (Feb 2008, Mar 2011 & Jan 2018) and 7a01634 is missing one survey
212 (Jan 2018). Topographic data are collected by the PCO using RTK-GPS with a quoted accuracy of ±
213 0.3 m (PCO, 2019c). LiDAR data were also acquired from the PCO, supplied as a 1 m grid with vertical
214 accuracy of 0.150 m (PCO, 2019a; Wiggins et al., 2019). All available LiDAR data from Crantock
215 beach were used, spanning from 2008 to 2016, with frequency of surveys varying between 6 months
216 and 2 years.
217

218 *2.3.2. UAV survey*

219 Two UAV surveys were conducted on 10th December 2018 and 26th June 2019 to capture the
220 morphological change over a winter season. Comparison with post-storm profile surveys shows that
221 there was limited change between the end of January and June 2019, and the UAV data therefore
222 represent the storm response over the 2018/19 winter, prior to post-winter recovery commencing. A
223 quadcopter UAV (DJI Phantom 4 Pro v2) with a 1'' CMOS sensor with 20M effective pixels was flown
224 at an altitude of 120 m. The flights were programmed using MapPilot with overlap and sidelap set to
225 80%. 30+ ground control points (GCPs) were spread across the study area to adequately represent the
226 variability in topography. GCP points were logged to ± 0.03 m vertical accuracy using Trimble R10
227 RTK-GPS (Real-Time Kinematic Global Positioning System). Using a 'Structure from Motion' (SfM)
228 approach (Turner et al., 2016; Westoby et al., 2012), overlapping aerial photographs were aligned and
229 georeferenced using the GCPs in Agisoft Metashape 1.5.3. A dense 3-D point cloud was generated (>50
230 points m^2), which was then interpolated to produce a 1-m digital elevation model (DEM).

231

232 ## 2.4. Assessing morphological response

233 *2.4.1. LiDAR and UAV*

234 DEMs were clipped and divided into 3 zones: dunes, intertidal, and river channel. Zone boundaries
235 were defined visually using 2008 Aerial Imagery from the PCO to assess the relative change from the
236 start of the time series. The UAV DEMs have a reduced extent due to survey restraints and were
237 primarily used for furthering the timeline of dune change. Geomorphic change analysis was conducted
238 by subtracting two overlapping DEM surfaces to produce a DEM of Difference (DoD) surface, with
239 each grid cell providing a value of the elevation change between the two DEMs (Wheaton et al., 2010).
240 The analysis was conducted using the Geomorphic Change Detection 7.4.1 add-in for ArcMap 10.6,
241 which enables thresholding of the change values to account for measurement uncertainty. Several
242 methods exist for propagating error through geomorphic change analysis (Bangen et al., 2016; Wheaton
243 et al., 2010), but here, a probabilistic approach was adopted (Brasington et al., 2003; Lane and Chandler,
244 2003). Under the assumption that the uncertainty of the DEMs (δz_{DEM}) is normally distributed, with a

reasonable approximation of DEM standard deviation of error (σ_{DEM}), it is possible to calculate a critical error threshold (U_{crit}) for each DoD grid point using:

$$U_{crit} = t\sqrt{(\sigma_{DEM1})^2 + (\sigma_{DEM2})^2} \quad (1)$$

where σ_{DEM1} and σ_{DEM2} are standard deviations for each DEM, and t is the critical student's t-value at a chosen confidence interval (Williams, 2012) where:

$$t = \frac{|Z_{DEM1} - Z_{DEM2}|}{\delta U_{DoD}} \quad (2)$$

where $|Z_{DEM1} - Z_{DEM2}|$ is the change in elevation of each cell in the DoD and δU_{DoD} is propagated uncertainty calculated by:

$$\delta U_{DoD} = \sqrt{(\delta z_{DEM1})^2 + (\delta z_{DEM2})^2} \quad (3)$$

The probability of the change occurring by measurement error can then be calculated by relating the *t*-value to its cumulative distribution function (Wheaton et al., 2010). Here a 95% confidence interval was used, where all elevation changes in the DoD below 95% confidence are thresholded out (Brasington et al., 2003; Wheaton et al., 2010; Wiggins et al., 2019). This methodology was applied using uncertainty values (δz_{DEM}) for LiDAR and UAV data of 0.15 m and 0.04, respectively, following (Wheaton et al., 2010; Wiggins et al., 2019).

2.4.2. Topographic profile analysis

The three profiles used here represent transects from the north (7a01643), central (7a01639) and south (7a01634) sections of the beach/dune system. Volumetric assessments were focused on the dune system, where only elevations above the toe of the dune were considered. The toe of the dune was defined as 5 m ODN (approximately 4.8 m above mean sea level), where a clear inflexion point exists. More involved methods to define toe elevation exist (Wernette et al., 2018); however, due to the variability in dune and beach slope over the time series, a consistent, albeit approximate toe position was used. Dune retreat was considered by calculating the centroid (centre of mass), tracking each profile's vertical and horizontal trajectory through time. The role of aeolian process in dune roll-over was assessed by calculating the amount of dune gain at the top or lee of the dunes over time.

2.5. Threshold analysis

In order to relate the boundary forcing conditions and the morphological response recorded at Crantock, a threshold analysis was conducted. Dune erosion at Crantock beach only occurs when high spring tides coincide with large waves, allowing swashes to reach the toe of the dune. As such, the number of hours above a significant wave height (H_s) threshold and water level (WL_{OD}) threshold were calculated per season, where winter is defined as November to March and summer as April to October. The threshold analysis was conducted using three scenarios:

1. Extreme waves and extreme water level – 5% exceedance H_s, WL_{OD} >/= MHWS;
2. Extreme waves and high water – 5% Exceedance H_s, WL_{OD} >/= MHW;
3. Extreme water level and high waves – 10% exceedance H_s, WL_{OD} >/= MHWS.

5% and 10% exceedance H_s values were 3.18 and 2.68 m, respectively, based on data from 2008 to 2019. MHWS and MHW are 3.40 and 2.55 m ODN (Ordnance Datum Newlyn), respectively. Data points were extracted where both thresholds were met, with each data point representing 30 minutes based upon the sampling frequency, which was summed to give total hours above combined threshold per season.

2.6. Numerical modelling

The process-based numerical model XBeach was used to investigate the dependence of dune erosion on initial beach morphology, and to test the hypothesis that the intertidal profile in front of the dune system altered by the changes in the River Gannel has been instrumental in causing the accelerated dune erosion. The aim was not to reproduce the observed dune erosion, but to look at the sensitivity of the dune response to the initial beach morphology; therefore, the model was not formally calibrated and validated.

XBeach can simulate wave propagation, wave induced currents, sediment transport, and morphological changes, solving the time-dependent short wave action-balance equations, roller energy equations, the non-linear shallow water equations of mass and momentum, sediment transport formulations, and bed

299 updating (Roelvink et al., 2015). In the 'surf beat' mode of XBeach used in this study, the variation of
300 the short-wave envelope is estimated on the scale of wave groups, an approach which is valid for
301 dissipative and intermediate beaches where swash motions are predominantly in the infragravity band,
302 and short waves are mostly dissipated by the time they reach the shore (Roelvink et al., 2018). The
303 XBeach model has proven to have a high level of predictive skill, particularly over the event timescale,
304 and has been shown to replicate observed impacts of storms on coastal dune systems (Bolle et al., 2011;
305 McCall et al., 2010; Splinter and Palmsten, 2012; Van Dongeren et al., 2009).
306 A sensitivity analysis was conducted in XBeach using the southern profile (7a01634) at four time-steps,
307 when the profile was in differing states:

308 1. January 2013 – before the 2013/14 storms;
309 2. March 2015 – before the first notable dune erosion phase;
310 3. October 2016 – before the second major dune erosion phase;
311 4. January 2019 – latest full survey to test the present vulnerability.

312
313 Due to a lack of subtidal surveys, each profile was merged with an offshore single-beam bathymetry
314 collected by the PCO in August 2007. A variable grid resolution was used in XBeach, using the Courant
315 number to optimise the grid spacing. A coarse resolution of 50 m was used at the offshore model
316 boundary (-20 m ODN), whilst at the coast the grid spacing was 1 m, ensuring a sufficient balance
317 between spatial resolution required and computational time.
318
319 Each simulation was run for 10 hours and the resultant erosion above the dune toe (at 5 m ODN) was
320 calculated. In addition to varying the starting profile as described above, H_s at the offshore boundary
321 was varied between 3 and 8 m with a fixed tide level of 4 m ODN (representing MHWS + 0.5 m storm
322 surge), and tide level was further varied between 2 and 6 m ODN with a fixed H_s of 4.2 m (1%
323 exceedance H_s). Mean values of wave direction and period from waves exceeding 1% H_s were
324 calculated and used in all simulations. A total of 80 simulations were run; Table 2 summarises the input
325 parameters used. All other model parameters were set to default with Morfac = 1.
326

3. Results

3.1. Forcing conditions

Summary plots of significant wave height (H_s), high tide water level (WL_{OD}), mean daily river discharge (Q) and wave direction are presented in Figure 2. The H_s time series (Figure 2a) shows a clear seasonal trend, with wave heights markedly higher on average over winter (H_s = 1.93 m) compared to lower average wave heights in summer (H_s = 1.23 m). The highest H_s measurements (> 6 metres) occurred in winter 2013/14 and 2017/18. The 8-week moving average of H_s reveals a more typical condition within each winter period, demonstrating that winter 2015/16 had relatively consistent high H_s, as well as demonstrating that, on average, the 2013/14 winter had the highest consistent peak in H_s. Wave direction (Figure 2d) is concentrated in a westerly direction, with an average wave angle of 282˚ (shore normal = 300˚) which also demonstrates limited seasonal or storm variability. Mean peak wave period (T_p) was 10.5 s but showed a similar seasonal variation to H_s, with longer mean T_p in winter and shorter mean T_p in summer.

Figure 2b displays the high tide sequence over the time series, displaying periods of exceptional high water when spring tides have combined with storm surge, predominantly in the winter months. The 2013/14 winter in particular shows a number of exceptional water levels, with very dense packing of peaks likely linked to the high number of storm surges that winter. The winters of 2012/13, 2014/15 and 2017/18 also show extreme periods of WL_{OD}. Daily mean discharge of the River Gannel (Figure 2c) shows extreme periods of discharge in winters, up to >10 m^3s^{-1} in winter 2012/13. As the Gannel has limited groundwater input, these peaks are linked with runoff during storms.

3.2. River Gannel channel migration

Results from the river Gannel planform change show that the river has had two distinct channel pathways (Figure 3). From March 2008 to March 2014 (and for potentially 100+ years preceding), the channel was pinned to the north Pentire Cliffs, reaching the sea at the most northerly point of the beach at MLWS. In the last few hundred metres of the river, there was evidence of lateral adjustments, but the

354 channel was mostly stable. From March 2016 until the most recent survey in June 2019, the channel
355 has avulsed, forming a new channel that flows along the beach and has much higher lateral variability.
356 The point at which the channel has avulsed was the location of an old training wall that initially held
357 the river in place from at least the early 1900s (Frith, 1928). Although there is a paucity of available
358 data during the year the channel switched, accounts from residents suggests it occurred in 2015 and,
359 therefore, it did not occur during the 2013/14 storms, as the data shows the channel was still in its
360 original position at the end of winter 2014 (Figure 3).
361

362 ## 3.2. Morphological response

363 ### *3.2.1. Qualitative changes to Crantock dunes*

364 Figure 4 shows a sequence of four aerial images of the Crantock dune system. Changes from 2001 to
365 2005 are mainly losses in vegetation cover, supposedly due to tourism pressures, but with limited
366 changes in the dune morphology apparent. The first two images also show extensive transport of sand
367 inland from the beach into the dune system, facilitated by wide dune ramps blanketing the underlying
368 bedrock. There is vegetation on the climbing dune deposits, but no vegetation on the slopes down to the
369 beach or above the high tide line, and there are no fore dunes present. This situation was also present in
370 2009 (not included due to poor image quality). The image taken in 2017 shows that the sand ramps have
371 almost completely been removed and the image taken in 2020 shows at some locations the underlying
372 bedrock (white dashed lines). The image taken in 2020 shows the steep dune face, practically a scarp,
373 indicated by the red dashed line in the image, but there does seem to be some indication that the dune
374 ramps are beginning to rebuild as a result of aeolian transport from the beach. The retreat over this 20-
375 year period is 40-50 m, but, as demonstrated later, most of this occurred over the period 2015–2019 (no
376 aerial images are available for the period 2009–2017).
377

378 ### *3.2.2. Volumetric change*

379 The geomorphic change analysis indicates that the intertidal region at Crantock was net erosional over
380 the from 2008 to 2016 (-54,290 ± 46,402 m^3). The dunes also experienced net erosion, which, due to

381 the additional surveys collected, is known to have continued to at least 2019 (-175,419 ± 22,287 m^3).
382 However, over the study period, the morphological response was quite variable over time and space.
383 Four primary epochs of change were observed: 2008–2012, 2012–2014, 2014–2016 and 2016–2019.
384 These epochs are distinguished by the spatial pattern of change observed, the position of the channel
385 and the dune response recorded (Figure 5). The full inter- and supra-tidal response within the
386 embayment across the four epochs is presented in Table 3.
387
388 From 2008 to 2012 (Epoch 1), Crantock shows relative stability, with evidence of overall accretion of
389 53,665 ± 28,142 m^3. Much of the accretion occurred in the intertidal zone, shown in Figure 5a as a band
390 of blue across the mid-beach, as well as some accretion at the toe of the dune. There was some evidence
391 of erosion in the dune zone; however, this was isolated to localised blowouts at the dune crest, and
392 accretionary zones are observed in the lee of the dune front surrounding the blowouts. Only the river
393 channel was net erosional over the study period; however, this was very marginal. Much of the erosion
394 in this epoch was focused around the channel/dune/beach interface, attributed to the lateral adjustment
395 of the river Gannel.
396
397 2012 to 2014 (Epoch 2) covers the major storms of winter 2013/14 and shows an almost reverse
398 response to Epoch 1, with the mid intertidal zone showing erosional losses and scarping at the toe of
399 the dune. There was some evidence of accretion in the lower intertidal region. Significant erosional
400 losses are made around the channel position on the beach, with a focused area around the training wall.
401 Despite some scarping of the toe of the dune, the dune system was relatively stable, as evidenced in
402 Figure 6. Overall, Epoch 2 shows a modest, and barely statistically significant, net sediment loss of -
403 40,233 ± 33,025 m^3.
404
405 2014 to 2016 (Epoch 3) shows more severe erosion of both the intertidal and dune areas than Epoch 2.
406 Notable areas of erosion appear in the upper intertidal and south end of the beach, while there was
407 evidence of a bar building at the north headland at the former location of the river channel, which
408 avulsed during this epoch. There was evidence of scarping of the dune toe during this epoch; however,

409 from Figure 6, it is clear that the dune volume had not yet significantly decreased below the 2008
410 volume. Conversely, the intertidal volume continued to decrease at a similar rate to that experienced
411 over Epoch 2, and dropped significantly below the 2008 volume. The River Gannel shows evidence of
412 channel shifting but maintains a stable sediment volume. Total loss over Epoch 3 was -93,962 ± 31,469
413 m^3.
414
415 In Epoch 4 (2016 to 2019), the overall net loss was -157,207 ± 16,368 m^3, which is higher than all three
416 previous epochs, despite the smaller survey area. The dunes and upper intertidal beach exhibit severe
417 levels of erosion, most notably at the south, with elevation differences of up to -16.5 m indicating an
418 extensive cutback of the high dune face. Results also show high levels of accretion in the lee of the
419 frontal dunes, suggesting an accelerated roll-over on the now bare dune faces. There was a mixed
420 response in the river Gannel area. The loss in dune volume during this period was extreme, equating to
421 a net loss of -126,604 ± 8,135 m^3.
422
423 The sediment volume time series for the intertidal, dune and river area is shown in Figure 6 and reveals
424 that, while the intertidal volume decreased sharply between 2012 and 2016, the dune volume did not
425 change significantly from the 2008 level until at least 2017, at which point it began to decline rapidly.
426 Despite the dramatic change in the river's position on the beach face, the river Gannel sediment volume
427 did not vary significantly over the study period.
428
429 *3.2.3. Profile change*
430 Figure 7 shows a time series of topographic profile data for the north, central, and south profiles between
431 2008 and 2019. There was a markedly different response at the north end of the beach to that of the
432 south end of the beach over the study period, with little dune erosion and a stable dune toe at the north,
433 compared to extreme dune erosion and toe retreat at the south end of the beach. There was a clear
434 gradient in erosional impact, with dune loss increasing further south along the dunes. Figure 7 reveals
435 that the distinctive dune retreat at the south and central profiles did not start until 2013 and was followed

436 by substantial cut-back during 2015 and 2017/18. In contrast, the northern profile, only 400 m away,
437 remained relatively stable during these events, and even experienced some toe progradation.
438
439 *3.2.4. Dune centroid change*
440 To further quantify the retreat of the dune, the centre of mass (or centroid) at each time step was
441 calculated (Figure 8). It is important to note that the dune centroid changes are not strictly
442 intercomparable between the three profiles, as the central and northern profiles cover a large area of
443 backdune, whilst the southern profile ends just behind the dune crest. Nevertheless, changes in the dune
444 centroid reveal how the overall position of the dune has evolved at each alongshore location. The
445 substantial increase in centroid elevation in the southern profile (4.9 metres) was driven by the
446 significant scarping of the dune toe, and signifies a narrowing of the dune base. The horizontal change
447 in the centre of mass indicates the overall retreat of the dune and is arguably more representative of
448 overall dune behaviour than considering the dune toe position alone. Annual averaged rates for dune
449 centroid retreat for the south, central and north profile are 2.3, 1.1 and 0.2 m yr^{-1}, respectively, but these
450 averaged rates mask the sporadic and at times extreme retreat that occurred. At the southern profile, the
451 dune centroid retreated 27 metres over the 11.5-year time series. Much of this change occurred in two
452 time-steps, from March 2015 to March 2016 and from October 2016 to March 2018, representing a
453 retreat of 13.5 and 12.5 metres respectively (Figure 8). The centre of mass in the central profile shows
454 a much lower magnitude of retreat over the time series (12.5 m). The central profile similarly shows a
455 stepped sequence of retreat however there are more steps evident but each with much smaller increments
456 of change (<5 m) than in the south. The north profile overall shows relative stability in the horizontal
457 and vertical position, with some oscillation seaward and landward and an overall retreat of just 2.5
458 metres over the time series.
459
460 ## 3.3. Comparison of environmental forcing to dune response
461 Volumetric change over time for each profile is presented in Figure 9a. The results quantify the major
462 erosional events witnessed on the southern profile as -208 m^3m^{-1} from March 2015 to March 2016, and

-521 m^3m^{-1} from October 2016 to March 2018. From the volumetric time series, a weaker erosional signal is shown in the central profile between October 2016 and March 2018. There was a mixed response between March 2015 and March 2016, with the central profile showing minor erosion and the northern profile showing minor accretion. Coherency in the response of the three profiles finally occurs between 2017 and 2018 when all three simultaneously lost sediment. In the years where a spring and autumn survey are present (2016, 2018 and 2019), a gradual recovery in sediment volumes was apparent following each winter; however, the magnitude of these recoveries was dwarfed by the large-scale erosion events.

There was a clear decoupling of dune erosion with environmental forcing conditions, as signified by a lack of alignment between periods of significant dune loss (Figure 9a) and periods featuring a large number of combined high wave and tide events (Figure 9b), which would be expected to drive dune erosion. Two outstanding seasons of combined high wave and water levels in winter 2013/14 and 2015/16 appear to have had a limited impact on the dune volumes, while, in contrast, significant dune losses occurred between October 2016 and March 2018 when the number of combined high wave and tide events was far fewer. This suggests that emergent behaviour might be influencing the dune evolution at Crantock.

3.4. Beach morphological control on dune erosion

Due to the lack of correlation between hydrodynamic forcing and dune erosion, the possibility that erosion has increased due to the river channel lowering the beach in front of the dune was considered. A series of 80 model runs were conducted in XBeach to test the sensitivity of dune response to the initial profile. Firstly, the modelling results (Figure 10) confirm that, for a given profile, dune erosion is enhanced by large waves and high-water levels. Predicted dune erosion increased by 1.5–2 times as the forcing wave height H_s was increased from 3 to 8 m (Figure 10e). Predicted dune erosion increased threefold as water level increased from MHWS to MHWS + 1.5 m (Figure 10f). However, there is also an evident sensitivity of dune erosion to starting morphology. While water level exerted the greatest

control on dune erosion overall, varying the starting profile resulted in a similar range of dune erosion to that caused by increasing the offshore wave height. The smallest beach volume (October 2016, 1967 m^3m^{-1}) resulted in a doubling of the dune erosion compared to the largest beach volume (January 2013, 2266 m^3m^{-1}), for each wave height considered. The initial morphology also showed increasing influence as water level was increased in the model.

Panels a-d in Figure 10 demonstrate the spatial pattern of modelled dune erosion for each of the four starting profiles, under a single set of forcing conditions (1% exceedance H_s = 4.2 m, water level just below the dune toe elevation = 4.5 m ODN). The January 2013 and March 2015 starting profiles (pre-river switch) are similar and result in comparable scarping at the dune toe and similar dune losses of -98 m^3m^{-1} and -110 m^3m^{-1}, respectively. These relatively modest dune losses can be attributed to the healthy intertidal beach volume and gently sloping dune face prior to the river switch, which enhance wave dissipation and reduce the vulnerability of the dune to slumping, respectively. The October 2016 starting profile (post-river switch) has a significantly lower intertidal profile fronting the dune than the earlier profiles due to the river cutting a parallel course in front of the dune, as well as a steepened dune face. This profile shows the most significant dune loss at -145 m^3m^{-1} under the modelled conditions. The January 2019 starting profile resulted in less dune loss (-118 m^3m^{-1}) than the 2016 profile, but is still impacted more than the pre-river switch profiles and exhibits erosion up to 25 metres elevation as the dune steepens even further, showing a severe vulnerability of the dune face.

The results also demonstrate that a large amount of sediment eroded from the dune accumulates in the sub- and inter-tidal zones, and it is likely that while the intertidal beach has been lowered by the presence of the river, the dune losses are starting to restore equilibrium by 'nourishing' the beach face and therefore helping to dissipate wave energy before it impacts the dunes. This may explain why the 2019 starting profile exhibits less dune loss than the 2016 profile despite the already steepened dune face, as it has a slightly higher intertidal volume.

4. Discussion

Firstly, it is essential to consider the environmental conditions over which this study is set. The hydrodynamic forcing time series from 2008 to 2019 is highly seasonal, but also shows inter-annual variability linked to extreme storm sequences. Central to this time frame is the unprecedented sequence of highly energetic wave events during the winter storms of 2013/14 (Masselink et al., 2016), which resulted in extensive morphological impacts along much of the European Atlantic coastline (Castelle et al., 2015; Masselink et al., 2015; Scott et al., 2016). Neighbouring beaches such as Perranporth, Watergate and Fistral experienced fairly dramatic intertidal and dune erosion during the storms, whilst Crantock showed modest losses to the beach face and toe of the dune. Previous explanations of a muted response from dune-backed beaches have linked this behaviour to an injection of large amounts of sediment onto the beach as a result of dune erosion (Burvingt et al., 2018), balancing out the overall sediment loss. However, Crantock shows only modest dune scarping during this period, despite the 2013/14 winter having the highest number of hours above the combined wave and tide hydrodynamic threshold (Figure 9b) in at least a decade. The reduced response may therefore be explained by Crantock's slightly reduced level of exposure (Burvingt et al., 2017), owing to its highly embayed shape and oblique orientation to the principal wave direction. Another notable difference between Crantock and other exposed north Cornish beaches has been in the recovery period following the 2013/14 storms. At highly exposed beaches, such as Perranporth and Watergate the sheer magnitude of the wave heights and periods took sediment far offshore to a deep-water bar (Scott et al., 2016), and as a result, energetic waves with long periods were required to bring sediment back onshore, resulting in a gradual, multi-annual recovery. Crantock on the other hand has experienced an acceleration in erosion since 2014, rather than gradual recovery.

Within the morphological response at Crantock, there is an apparent delay between the erosional loss experienced on the beach, initiated by the 2013/14 storms and the erosion in the dune system, which begins to occur over the 2015/16 winter. There are two distinct phases of dune erosion recorded in the time series, the initial phase between March 2015 and March 2016 is only really experienced at the

544 southern end of the dune system (-208 m^3m^{-1}), with the central dunes showing minor erosion (-44 m^3m^{-1}) and the northern dunes showing a net accretion (+76 m^3m^{-1}). The same north-south gradient is somewhat evident in the second erosion phase (October 2016 to March 2018); however, the magnitude is significantly higher (-520 m^3m^{-1} in the south, -183 m^3m^{-1} in the central dunes, and -127 m^3m^{-1} in the north), despite the lower hydrodynamic forcing over this period. The rate of dune retreat is very significant with an along-coast averaged dune retreat over the period 2008-2019 of 2.3 myr^{-1}, and much of this retreat happening in the two erosional phases identified. In comparison to other sites (Castelle et al., 2015; Scott et al., 2016; Suanez et al., 2015), the dune erosion experienced at Crantock shows equal or higher magnitudes of change but has occurred over a period with significantly lower hydrodynamic forcing. The results demonstrate that the first hypothesis, that the acceleration in dune erosion is directly linked to the hydrodynamic forcing (wave, tide or river discharge), can be rejected.

555

556 The second hypothesis presented here is that the switching of the River Gannel between March 2014 and March 2016, resulted in a lowering of the beach and subsequently accelerated dune erosion. The winter of 2014/15 saw particularly low energy wave conditions, resulting in more constructive waves returning sediment onshore. From Figure 5c, it is clear that the sediment accumulates in the old channel position, meaning higher amounts of fluvial energy would be required for the channel to retain its pathway. During the same winter, the Gannel exhibited significantly low discharge, thus making the river more amenable to a forced avulsion. During low flows the river is less likely to keep up with the sediment accumulation from constructive waves, and combined with the degradation of the training wall, the channel shifted to find the path of least resistance, leading the river to flow across the beach. A lower beach elevation increases the depth of water at the toe of the dune during a storm event that coincides with MHWS, meaning large waves with higher energy can act upon the dune face (Armaroli et al., 2012; Cooper et al., 2007). As a result, even weaker magnitude winters, can produce a disproportionately large response in dune erosion. The lower beach level results in a higher amount of basal wetting and undercutting, increasing the risk of avalanche failure (Carter and Stone, 1989). As a result of the channel avulsion and a subsequently persistent wet beach face, it is likely that aeolian transport and therefore dune recovery has been hindered. The high dunes at Crantock have likely

572 developed due to the river being pinned against the north headland from the early 1900s, at least,
573 according to historical imagery (Frith, 1928), allowing the beach face to dry out more frequently and
574 aeolian processes to develop the dunes over a 100+ year period.
575
576 1-D XBeach model runs, using two fixed hydrodynamic conditions on four different initial beach
577 profiles, indicate a clear sensitivity of dune erosion to beach level, with a markedly different volumetric
578 and cross-sectional result following the modelled storm event. This dependency of dune erosion
579 magnitudes on beach morphology has been recorded previously in modelling of storm clustering effects
580 on dunes (Dissanayake et al., 2015; Splinter et al., 2014), where proceeding storms in a cluster can have
581 a reduced impact than anticipated as the morphology adjusts. The reduced magnitude of the January
582 2019 dune erosion volume may be explained by the shift of the toe of the dune higher and further
583 landward than that of March 2016, reducing the access to the dune of the subsequent storm (Dissanayake
584 et al., 2015). Pre-storm beach swash slope has been shown to play a significant role in determining
585 relative dune erosion (Splinter et al., 2014). The results presented here support the importance of beach
586 morphology in controlling dune erosion; however, in this case, beach morphology is further modified
587 by a switching river channel rather than solely antecedent hydrodynamics. More broadly for coastal
588 modelling applications, the results presented here highlight the sensitivity of beach and dune response
589 in a given model to the starting profile, emphasising a need to correctly select or test the initial beach
590 morphology before a given model is run.
591
592 Crantock beach and dune system show an emergent geomorphic response, where it is evident that the
593 sum of the apparent environmental processes are disproportionate to the morphological outcome
594 observed (Favis-Mortlock, 2013; Phillips, 2003). In the years following the major 2013/14 winter storm
595 sequence, when a recovery of the intertidal zone was expected, the river Gannel avulsed, resulting in
596 the unexpected contingent outcome of extreme dune erosion. The interaction between fluvial, aeolian
597 and coastal processes resulted in highly localised erosion, with a severe magnitude in the southern dunes
598 at Crantock. The results presented here demonstrate that underlying the complexity of the geomorphic
599 response observed at Crantock there is generative simplicity, with the overall response attributed to a

sequence of simple, local interactions between the river channel, beach and dune system. The concepts of emergence and complexity have been more widely adopted in fluvial geomorphology but remain relatively underutilised in coastal morphodynamic literature. Particularly in such interconnected geomorphological systems such as Crantock Beach, it is crucial to look beyond a simple reductionist approach. Crantock is a prime example of an emergent behaviour in coastal geomorphology where the formation of the whole-system output is surprising – a dune system experiencing extreme erosion that appears decoupled from the hydrodynamic forcing.

There are relatively few studies showing similar dune and river mouth dynamics from other beach systems. However, across the local region alone, similar processes may have occurred at the Hayle and Camel estuaries (Cornwall, UK), which both have rivers adjacent to eroding sand dunes. For example, at the Hayle Estuary, an end to sluicing of the deep-water channel for navigation has resulted in a significant change to the estuary morphology, allowing sand accumulation in the mouth of the estuary and subsequently a narrower and more variable river mouth position that has altered the tidal prism and influenced sediment transport rates adjacent to the rivermouth (Golowyn, 2004; Penwith District Council, 2002). The response at Hayle and Crantock beaches to changes in river geometry highlight the sensitivity of sandy dune systems to nearby fluvial processes, especially where some form of human intervention has taken place to modify the river dynamics.

5. Conclusion

This study presents an interpretive and open-ended geomorphic analysis into the emergent behaviour of a climbing dune system at Crantock Beach, north Cornwall. In the subsequent years following the major 2013/14 storms, where extreme erosion was observed across the South West of England, the morphological response of the dunes at Crantock appears to have become decoupled from hydrodynamic forcing with the most significant cutbacks in relatively low winter wave-tide conditions. The onset of extreme dune erosion at Crantock can be attributed by the shifting River Gannel that has

its outflow on the beach. Shifting intertidal sediment during the recovery of the 2013/14 storms, combined with a degradation of the training wall, allowed the river to freely migrate across the beach. XBeach modelling reveals that the shifting river channel resulted in a lowering of the beach level, which has increased the vulnerability of the dunes and resulted in extreme dune erosion.

Acknowledgments

The author would like to thank all those who assisted with UAV surveys at Crantock beach: Aikaterini Konstantinou, Craig Dornan, Bethany Reed, Rachel Combes, Tim Poate, and in particular Peter Ganderton who piloted the surveys. Thanks go to Ian Kemp, Mike Simmonds, Lucy Smith and Tony Flux at the National Trust for approving and assisting with the planning of the UAV surveys. Additional data was provided by the Plymouth Coastal Observatory (PCO) containing public sector information licensed under the Open Government License v3.0. This work was funded by the UK Natural Environment Research Council under grant NE/M004996/1 (BLUE-coast project).

References

Arens, S.M., 1997. Transport rates and volume changes in a coastal foredune on a Dutch Wadden island. Journal of Coastal Conservation 3, 49-56.

Armaroli, C., Ciavola, P., Perini, L., Calabrese, L., Lorito, S., Valentini, A., Masina, M., 2012. Critical storm thresholds for significant morphological changes and damage along the Emilia-Romagna coastline, Italy. Geomorphology 143, 34-51.

Bangen, S., Hensleigh, J., McHugh, P., Wheaton, J., 2016. Error modeling of DEMs from topographic surveys of rivers using fuzzy inference systems. Water Resources Research 52, 1176-1193.

BBC, 2018. Climbing Cornish sand cliffs 'could kill instantly'.

Bolle, A., Mercelis, P., Roelvink, D., Haerens, P., Trouw, K., 2011. Application and validation of XBeach for three different field sites. Coastal Engineering Proceedings 1, 1-13.

Brasington, J., Langham, J., Rumsby, B., 2003. Methodological sensitivity of morphometric estimates of coarse fluvial sediment transport. Geomorphology 53, 299-316.

654 Bruun, P., 1962. Sea-level rise as a cause of shore erosion. Journal of the Waterways and Harbors
655 division 88, 117-132.
656 Burvingt, O., Masselink, G., Russell, P., Scott, T., 2017. Classification of beach response to
657 extreme storms. Geomorphology 295, 722-737.
658 Burvingt, O., Masselink, G., Scott, T., Davidson, M., Russell, P., 2018. Climate forcing of
659 regionally-coherent extreme storm impact and recovery on embayed beaches. Marine Geology 401,
660 112-128.
661 Buscombe, D.D., Scott, T.M., 2008. The Coastal Geomorphology of North Cornwall: St Ives
662 Head to Trevose Head. Wave hub Impact on Seabed and Shoreline Processes (WHISSP). University of
663 Plymouth.
664 Carter, R.W.G., 2013. Coastal environments: an introduction to the physical, ecological, and
665 cultural systems of coastlines. Academic Press, San Diego, California.
666 Carter, R.W.G., Stone, G.W., 1989. Mechanisms associated with the erosion of sand dune cliffs,
667 Magilligan, Northern Ireland. Earth Surface Processes and Landforms 14, 1-10.
668 Castelle, B., Dodet, G., Masselink, G., Scott, T., 2018. Increased winter-mean wave height,
669 variability, and periodicity in the Northeast Atlantic over 1949–2017. Geophysical Research Letters 45,
670 3586-3596.
671 Castelle, B., Marieu, V., Bujan, S., Splinter, K.D., Robinet, A., Sénéchal, N., Ferreira, S., 2015.
672 Impact of the winter 2013–2014 series of severe Western Europe storms on a double-barred sandy coast:
673 Beach and dune erosion and megacusp embayments. Geomorphology 238, 135-148.
674 Church, J.A., Clark, P.U., Cazenave, A., Gregory, J.M., Jevrejeva, S., Levermann, A., Merrifield,
675 M.A., Milne, G.A., Nerem, R.S., Nunn, P.D., Payne, A.J., Pfeffer, W.T., Stammer, D., Unnikrishnan,
676 A.S., 2013. Sea Level Change, in: Stocker, T.F., Qin, D., Plattner, G.-K., Tignor, M., Allen, S.K.,
677 Boschung, J., Nauels, A., Xia, Y., V., B., Midgley, P.M. (Eds.), Climate Change 2013: The Physical
678 Science Basis. Contribution of Working Group I to the Fifth Assessment Report of the
679 Intergovernmental Panel on Climate Change. . Cambridge University Press, Cambridge, UK, pp. 1137-
680 1216.

Christiansen, M. and Davidson-Arnott, R., 2004. The effects of dune ramps on sediment supply to coastal foredunes, Skallingen Denmark. Geografisk Tidskrift, 104, 29-41.

Cooper, J.A.G., McKenna, J., Jackson, D.W.T., O'Connor, M., 2007. Mesoscale coastal behavior related to morphological self-adjustment. Geology 35, 187-190.

Davies, H.C., 2015. Weather chains during the 2013/2014 winter and their significance for seasonal prediction. Nature Geoscience 8, 833.

Dissanayake, P., Brown, J., Wisse, P., Karunarathna, H., 2015. Comparison of storm cluster vs isolated event impacts on beach/dune morphodynamics. Estuarine, Coastal and Shelf Science 164, 301-312.

Doyle, T.B., Short, A.D., Ruggiero, P., Woodroffe, C.D., 2019. Interdecadal Foredune Changes along the Southeast Australian Coastline: 1942–2014. Journal of Marine Science and Engineering 7, 177.

EA, 2019. Environment Agency Hydrological Data.

Edelman, T., 1969. Dune erosion during storm conditions, 11th International Conference on Coastal Engineering, London, United Kingdom, pp. 719-722.

Everard, M., Jones, L., Watts, B., 2010. Have we neglected the societal importance of sand dunes? An ecosystem services perspective. Aquatic Conservation: Marine and Freshwater Ecosystems 20, 476-487.

Express, 2019. 'A matter of time!' Coastguard fury as children pose on cliff-edge DAYS after landslide.

Favis-Mortlock, D., 2013. 1.14 Systems and Complexity in Geomorphology, in: Shroder, J., Orme, A.R., Sack, D. (Eds.), Treatise in Geomorphology. Academic Press, San Diego, California, pp. 257-270.

Frith, F., 1928. Crantock, River Gannel And West Pentire 1928.

Gallagher, R., Appenzeller, T., 1999. Beyond reductionism. Science 284, 79-80.

Golowyn, M., 2004. Investigation of beach change at Hayle, Cornwall. PhD Dissertation, University of Plymouth.

Guisado-Pintado, E., Jackson, D.W.T., 2019. Coastal impact from high-energy events and the importance of concurrent forcing parameters: the cases of Storm Ophelia (2017) and Storm Hector (2018) in NW Ireland: Coastal impact from high-energy events and the importance of concurrent forcing parameters. Frontiers in Earth Science 7, 190.

Harrison, S., 2001. On reductionism and emergence in geomorphology. Transactions of the Institute of British Geographers 26, 327-339.

Hesp, P. A., 2005. Flow reversal and dynamics of foredunes and climbing dunes on a Leeward East Coast, New Zealand. Zeitschrift fur Geomorphologie, Supplementband, 141, 123-134.

Ho, L.-D., Luthgens, C., Wong, Y.-C., Yen, J.-Y. and Chyi, S.-J., 2017. Late Holocene cliff-top dune evolution in the Hengchun Peninsula of Taiwan: Implications for palaeoenvironmental reconstruction, Journal of Asian Earth Sciences, 148, 13-30.

Houser, C., Hapke, C., Hamilton, S., 2008. Controls on coastal dune morphology, shoreline erosion and barrier island response to extreme storms. Geomorphology 100, 223-240.

Jackson, N.L., Nordstrom, K.F., 1997. Effects of time-dependent moisture content of surface sediments on aeolian transport rates across a beach, Wildwood, New Jersey, USA. Earth Surface Processes and Landforms 22, 611-621.

Konstantinou, A., Stokes, C., Masselink, G. and Scott, T., 2021. The extreme 2013/14 winter storms: Regional patterns in multi-annual beach recovery. *Geomorphology*, 107828.

Lane, S.N., Chandler, J.H., 2003. The generation of high quality topographic data for hydrology and geomorphology: new data sources, new applications and new problems. Earth surface processes and landforms: the journal of the British Geomorphological Research Group 28, 229-230.

Masselink, G., Castelle, B., Scott, T., Dodet, G., Suanez, S., Jackson, D., Floc'h, F., 2016. Extreme wave activity during 2013/2014 winter and morphological impacts along the Atlantic coast of Europe. Geophysical Research Letters 43, 2135-2143.

Masselink, G., Scott, T., Poate, T., Russell, P., Davidson, M., Conley, D., 2015. The extreme 2013/2014 winter storms: hydrodynamic forcing and coastal response along the southwest coast of England. Earth Surface Processes and Landforms 41, 378-391.

McCall, R.T., De Vries, J.V.T., Plant, N., Van Dongeren, A., Roelvink, J., Thompson, D., Reniers, A., 2010. Two-dimensional time dependent hurricane overwash and erosion modeling at Santa Rosa Island. Coastal Engineering 57, 668-683.

Murray, A.B., Coco, G., Goldstein, E.B., 2014. Cause and effect in geomorphic systems: complex systems perspectives. Geomorphology 214, 1-9.

Murray, A.B., Lazarus, E., Ashton, A., Baas, A., Coco, G., Coulthard, T., Fonstad, M., Haff, P., McNamara, D., Paola, C., 2009. Geomorphology, complexity, and the emerging science of the Earth's surface. Geomorphology 103, 496-505.

Nordstrom, K.F., Jackson, N.L., 2012. Physical processes and landforms on beaches in short fetch environments in estuaries, small lakes and reservoirs: a review. Earth-Science Reviews 111, 232-247.

NRFA, 2019. 49004 - Gannel at Gwills Station Info.

Oyedotun, T.D.T., 2014. Shoreline geometry: DSAS as a tool for Historical Trend Analysis, in: Clarke, L., Nield, J.M. (Eds.), Geomorphological Techniques. British Society for Geomorphology, London, UK.

Oyedotun, T.D.T., 2015. Estuary – coast interaction and morphodynamic evolution: a comparative analysis of three estuaries in southwest England. University College London.

Palmer, M., Howard, T., Tinker, J., Lowe, J., Bicheno, L., Calvert, D., Edwards, T., Gregory, J., Harris, G., Krijnen, J., Pickering, M., Roberts, C., Wolf, J., 2018. UKCP18 Marine Report, UK Climate Projections. Met Office, London, UK.

PCO, 2019a. LiDAR.

PCO, 2019b. South West Regional Coastal Monitoring Programme.

PCO, 2019c. Topographic Surveys.

Penwith District Council, 2002. Hayle Harbour hydrondynamic modelling report. Babtie Group, Glasgow.

Phillips, J.D., 2003. Sources of nonlinearity and complexity in geomorphic systems. Progress in Physical Geography 27, 1-23.

Phillips, J.D., 2011. Emergence and pseudo-equilibrium in geomorphology. Geomorphology 132, 319-326.

763 Phillips, J.D., 2014. State transitions in geomorphic responses to environmental change.
764 Geomorphology 204, 208-216.
765 Pye, K., Neal, A., 1994. Coastal dune erosion at Formby Point, north Merseyside, England:
766 causes and mechanisms. Marine Geology 119, 39-56.
767 Pye, K.S., Samantha; Blott, Simon, 2007. Sand dune processes and management for flood and
768 coastal defence Joint Defra/EA Flood and Coastal Erosion Risk Management R&D Programme Joint
769 Defra/EA Flood and Coastal Erosion Risk Management R&D Programme
770 Radley, G.P., 1994. Sand Dune Vegetation Survey of Great Britain: Part 1 – England. Report by
771 English Nature for Joint Nature Conservation Committee, 126 pp.
772 Roelvink, D., McCall, R., Mehvar, S., Nederhoff, K., Dastgheib, A., 2018. Improving predictions
773 of swash dynamics in XBeach: The role of groupiness and incident-band runup. Coastal Engineering
774 134, 103-123.
775 Roelvink, D., Van Dongeren, A., McCall, R., Hoonhout, B., Van Rooijen, A., Van Geer, P., de
776 Vet, L., Nederhoff, K., 2015. XBeach model description and manual. Deltares, UNESCO-IHE Institute
777 of Water Education and Delft University of Technology, The Netherlands.
778 Scott, T., Masselink, G., O'Hare, T., Saulter, A., Poate, T., Russell, P., Davidson, M., Conley, D.,
779 2016. The extreme 2013/2014 winter storms: Beach recovery along the southwest coast of England.
780 Marine Geology 382, 224-241.
781 Scott, T., Masselink, G., Russell, P., 2011. Morphodynamic characteristics and classification of
782 beaches in England and Wales. Marine Geology 286, 1-20.
783 Splinter, K.D., Carley, J.T., Golshani, A., Tomlinson, R., 2014. A relationship to describe the
784 cumulative impact of storm clusters on beach erosion. Coastal Engineering 83, 49-55.
785 Splinter, K.D., Palmsten, M.L., 2012. Modeling dune response to an East Coast Low. Marine
786 Geology 329, 46-57.
787 Suanez, S., Cancouët, R., Floc'h, F., Blaise, E., Ardhuin, F., Filipot, J.-F., Cariolet, J.-M.,
788 Delacourt, C., 2015. Observations and predictions of wave runup, extreme water levels, and medium-
789 term dune erosion during storm conditions. Journal of Marine Science and Engineering 3, 674-698.

790 Turner, I.L., Harley, M.D., Drummond, C.D., 2016. UAVs for coastal surveying. Coastal
791 Engineering 114, 19-24.
792 Tătui, F., Vespremeanu-Stroe, A., Preoteasa, L., 2014. Alongshore variations in beach-dune
793 system response to major storm events on the Danube Delta coast. Journal of Coastal Research 70, 693-
794 700.
795 Van Dongeren, A., Bolle, A., Vousdoukas, M.I., Plomaritis, T., Eftimova, P., Williams, J.,
796 Armaroli, C., Idier, D., Van Geer, P., Van Thiel de Vries, J., 2009. MICORE: dune erosion and
797 overwash model validation with data from nine European field sites, Proceedings Of Coastal Dynamics
798 2009: Impacts of Human Activities on Dynamic Coastal Processes. World Scientific, pp. 1-15.
799 van Thiel de Vries, J.S.M., Van Gent, M.R.A., Walstra, D.J.R., Reniers, A., 2008. Analysis of
800 dune erosion processes in large-scale flume experiments. Coastal Engineering 55, 1028-1040.
801 Vellinga, P., 1982. Beach and dune erosion during storm surges. Coastal Engineering 6, 361-387.
802 Wernette, P., Thompson, S., Eyler, R., Taylor, H., Taube, C., Medlin, A., Decuir, C., Houser, C.,
803 2018. Defining Dunes: Evaluating How Dune Feature Definitions Affect Dune Interpretations from
804 Remote Sensing. Journal of Coastal Research 34, 1460-1470.
805 Westoby, M.J., Brasington, J., Glasser, N.F., Hambrey, M.J., Reynolds, J.M., 2012. 'Structure-
806 from-Motion' photogrammetry: A low-cost, effective tool for geoscience applications. Geomorphology
807 179, 300-314.
808 Wheaton, J.M., Brasington, J., Darby, S.E., Sear, D.A., 2010. Accounting for uncertainty in
809 DEMs from repeat topographic surveys: improved sediment budgets. Earth surface processes and
810 landforms: the journal of the British Geomorphological Research Group 35, 136-156.
811 Wiggins, M., Scott, T., Masselink, G., Russell, P., McCarroll, R.J., 2019. Coastal embayment
812 rotation: Response to extreme events and climate control, using full embayment surveys.
813 Geomorphology 327, 385-403.
814 Williams, R.D., 2012. Section 2.3. 2: DEMs of difference, in: Cook, S.J.C., L . E., Nield, J. M.
815 (Ed.), Geomorphological Techniques (Online Edition). British Society for Geomorphology, London,
816 UK.

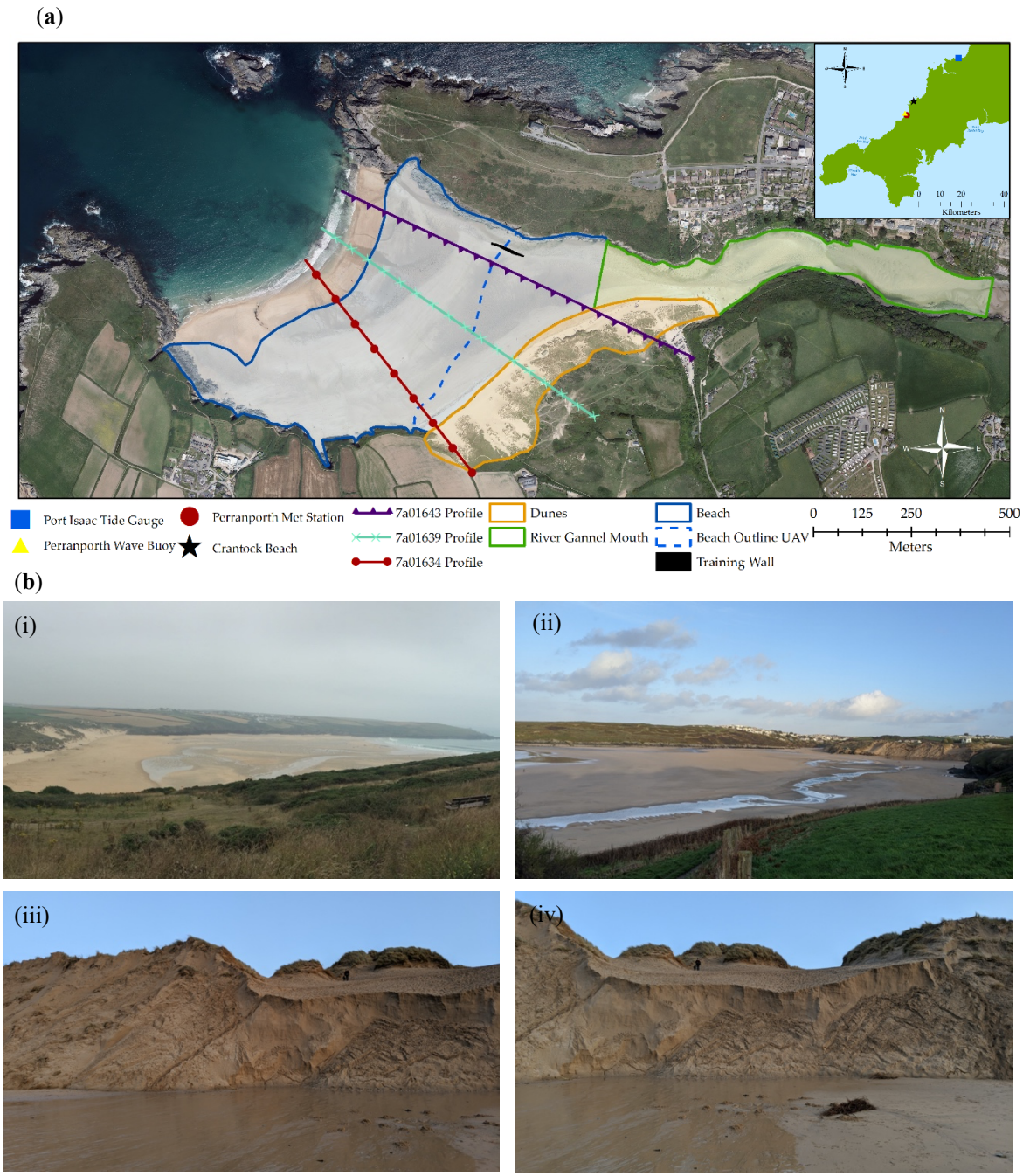

Figure 1. (**a**) Location Map of Crantock beach with survey profiles (Plymouth coastal Observatory profile codes) and polygons highlighted. Aerial photograph from 5th May 2013 (PCO, 2019b). Port Isaac Tide gauge, Perranporth Wave Buoy and Meteorological station are highlighted in the regional map. (**b**) Photographs of Crantock beach taken in (i) August 2016 and (ii-iv) January 2020 by Christopher Stokes.

Table 1. Topographic survey data acquired to assess the morphological response at Crantock.

	Year											
Survey Data	**2008**	**2009**	**2010**	**2011**	**2012**	**2013**	**2014**	**2015**	**2016**	**2017**	**2018**	**2019**
Profiles[1,2]	Feb			Mar	Jun	Jan	Mar	Mar	Mar		Jan, Mar	Jan
LiDAR[1]	Mar	Mar	Oct		Apr		Mar		Mar, Oct			
UAV											Dec	Jun

[1] Data provided by the PCO.

[2] Profile data is supplemented with profiles extracted from LiDAR and UAV datasets.

Table 2. XBeach input parameters for sensitivity analysis of beach lowering on dune erosion.

Input Parameter	**Values (min: increment:max)**	**Explanation**
Wave Height (H_S)	3:0.5:8 m, and 4.2 m	Storm wave heights, and 1% exceedance H_s
Water Level	2:0.5:6 m ODN	MHWS - 1.5 m to MHWS + 2.5 m
Wave Period (T_p)	12.5 s	Mean storm wave period.
Wave Angle	285˚	Mean storm wave angle.
Grain Size	0.28 mm	D_{50} value.

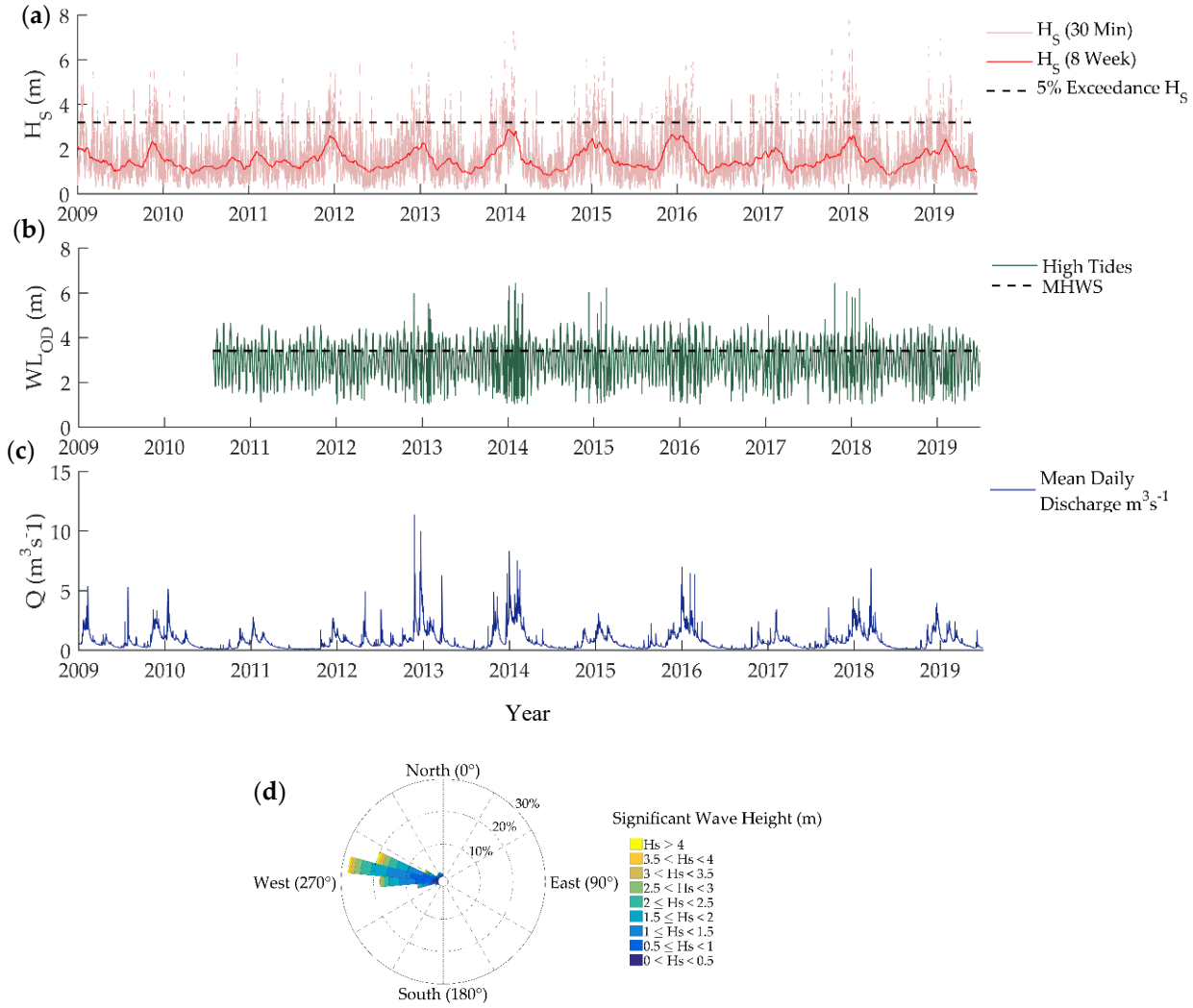

Figure 2. Environmental boundary conditions over the study period. (**a**) Significant wave height (H_S) measured by the Perranporth Wave Buoy in ~14-m depth, overlaid with an 8-week moving average and 5% exceedance threshold. (**b**) High tide water elevation (WL_{OD}) with MHWS threshold (3.4 m ODN). (**c**) Daily mean discharge from the River Gannel (Q). (**d**) Summary of wave directionality.

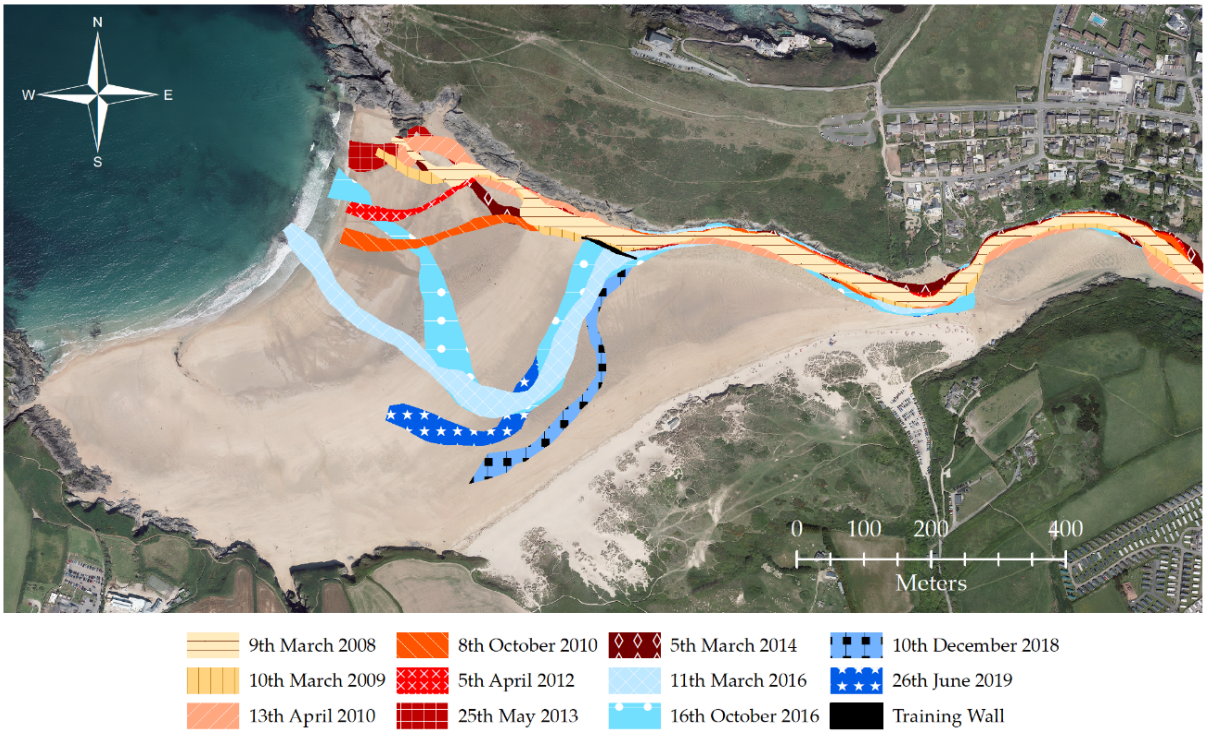

Figure 3. River Gannel planform change from 2008 to 2019 and the location of the training wall. Digitised in ArcMap 10.6 using LiDAR, aerial photographs and UAV data. Overlaid onto 2013 aerial photographs from the PCO.

Table 3. Summary of morphological response at Crantock beach between 2008 and 2019.

		Net Sediment Volume Change (m^3)			
Epoch	**Description**	**Dunes**	**Intertidal**	**River Gannel**	**Total**
1. 2008–2012	Stable and some accretion on the beach and toe of dunes. Minor erosion in channel.	+16,376 ±7,097 m^3	+42,833 ±18,579 m^3	-5,545 ±2,466 m^3	+53,665 ±28,142 m^3
2. 2012–2014	Erosion on beach and toe of dunes, accretion in the channel.	-6,004 ±4,542 m^3	-53,889 ±25,623 m^3	+19,659 ±4,860 m^3	-40,233 ±33,025 m^3
3. 2014–2016	Continuation of beach erosion and accelerated erosion of dunes. Minor erosion in channel.	-24,203 ±5,539 m^3	-65,081 ±23,348 m^3	-4,678 ±2,583 m^3	-93,962 ±31,469 m^3
4. 2016–2019[1]	Severe erosion in dunes and top of the beach, a mixed response in river Gannel mouth.	-126,604 ±8,135 m^3	-27,166 ±5,348 m^3	-3,436 ±2,885 m^3	-157,206 ±16,368 m^3

[1] 2016-2019 epoch has reduced coverage of the Intertidal and River Gannel. Only the Dune polygon is fully surveyed.

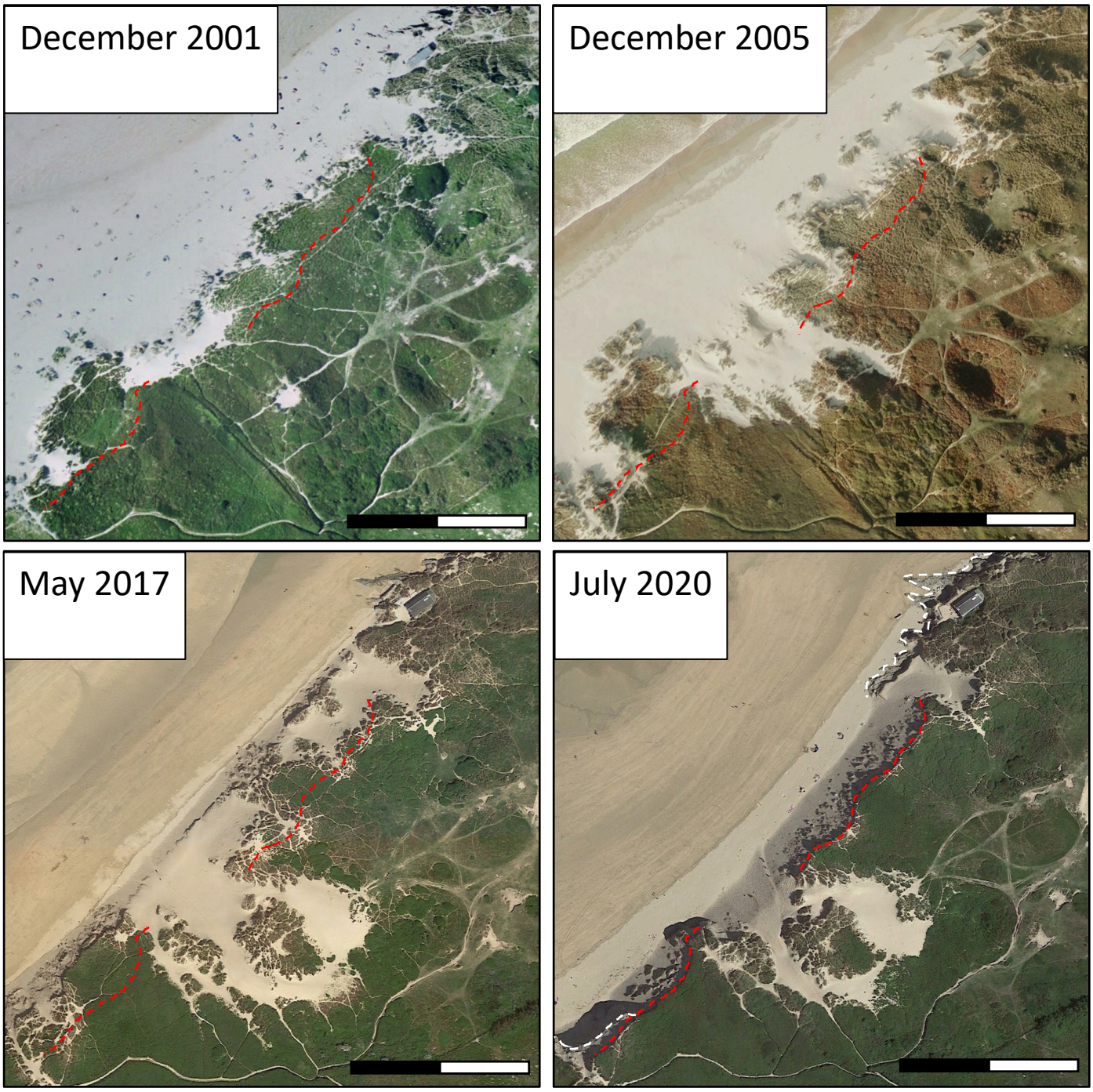

Figure 4. Aerial photographs showing the evolution of the Crantock dunes from 2001 to 2020 (GoogleEarth). The red dashed line in the top-left panel represents the seaward edge of the vegetated dune in 2020, shown in the bottom-right panel. The white dashed lines in the bottom-right panel represents where bedrock outcrops on the beach. The scale bar represent 100 m.

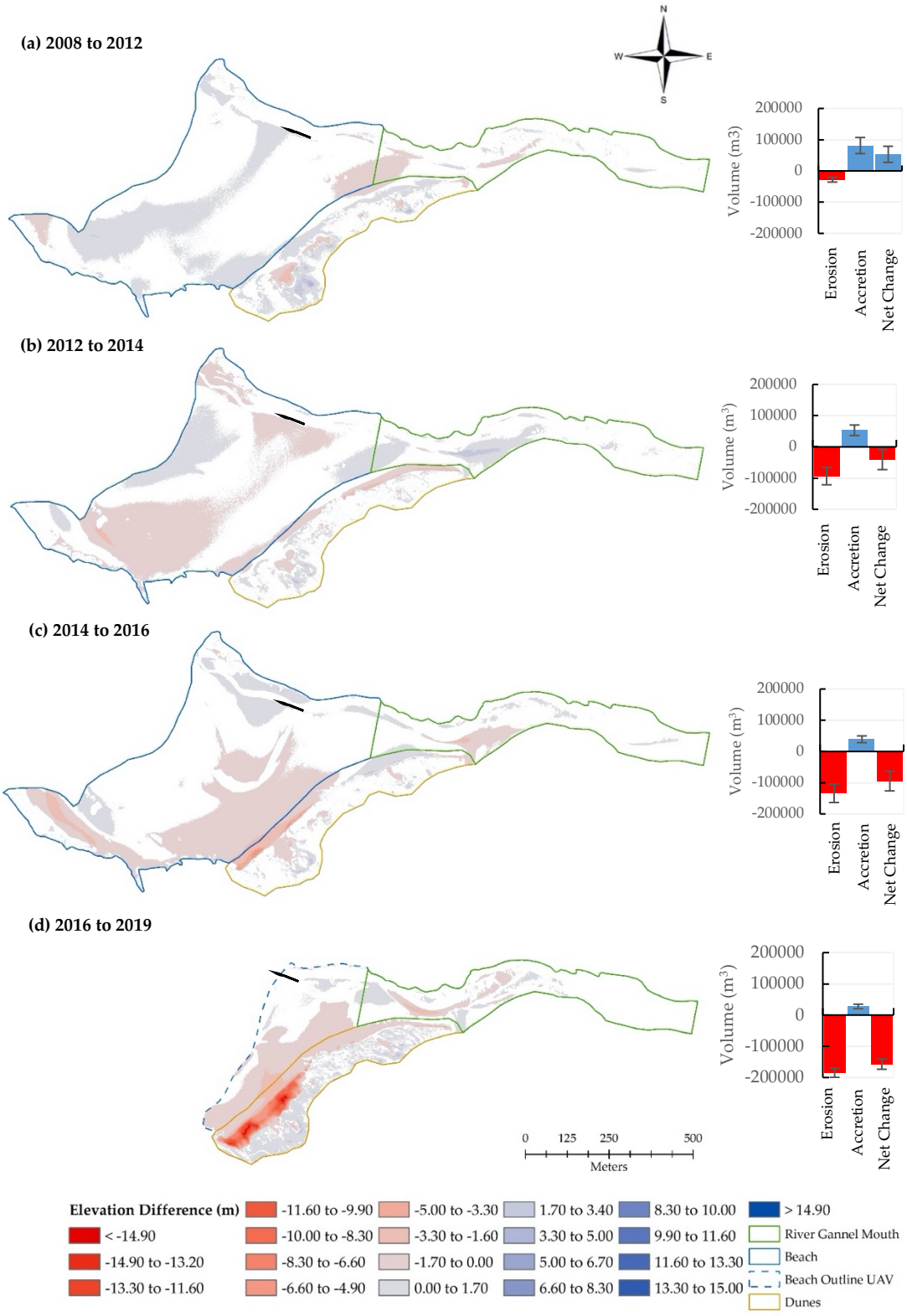

Figure 5. Morphological response of Crantock beach over 4 epochs: (**a**) 2008–2012; (**b**) 2012–2014; (**c**) 2014–2016; (**d**) 2016–2019. The bar graphs represent volumetric change across the entire survey area for each epoch. Change in elevation is represented by different colour intensities of red (erosion) and blue (accretion), where an absence of colour shows no detectable change above the 95% probabilistic threshold.

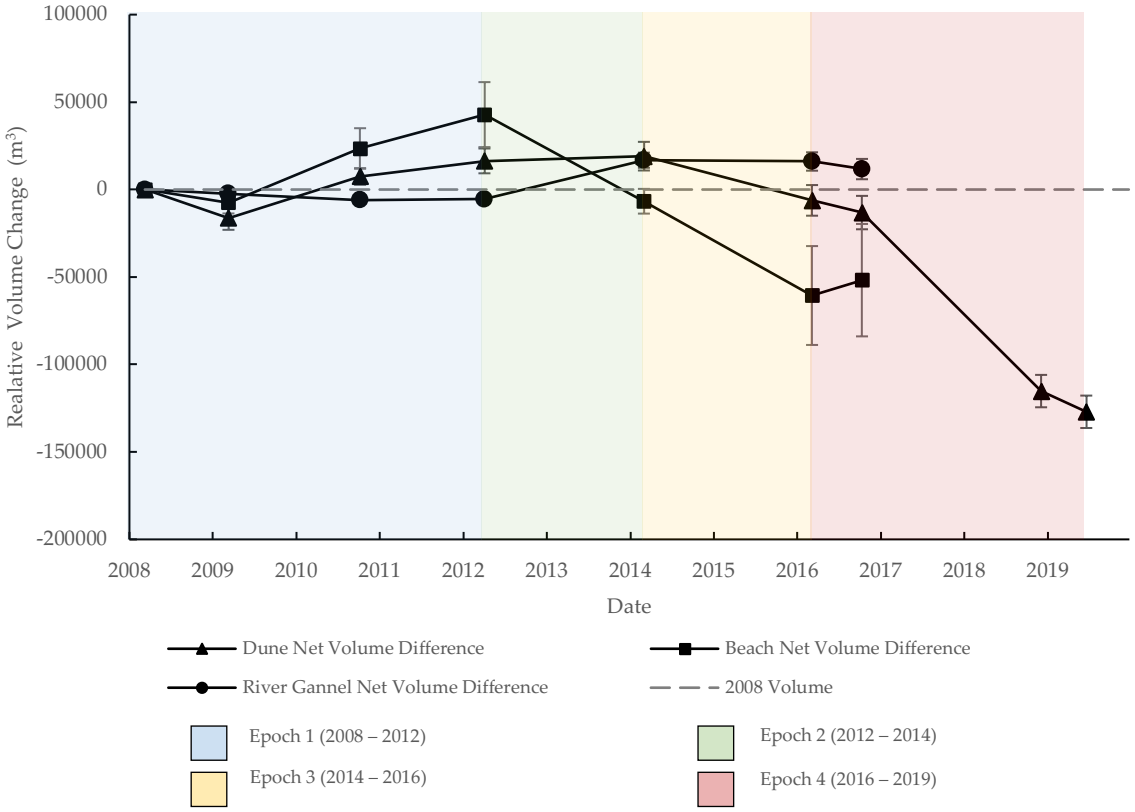

Figure 6. Volume time series from 3 zones at Crantock Beach: Dune (triangles), Intertidal (squares) and River Gannel Channel (circles). Black lines represent the net volume difference relative to the first survey on 9th March 2008. LiDAR data until 16/10/2016 with additional UAV data on 10/12/2018 and 26/06/2019 (dunes only).

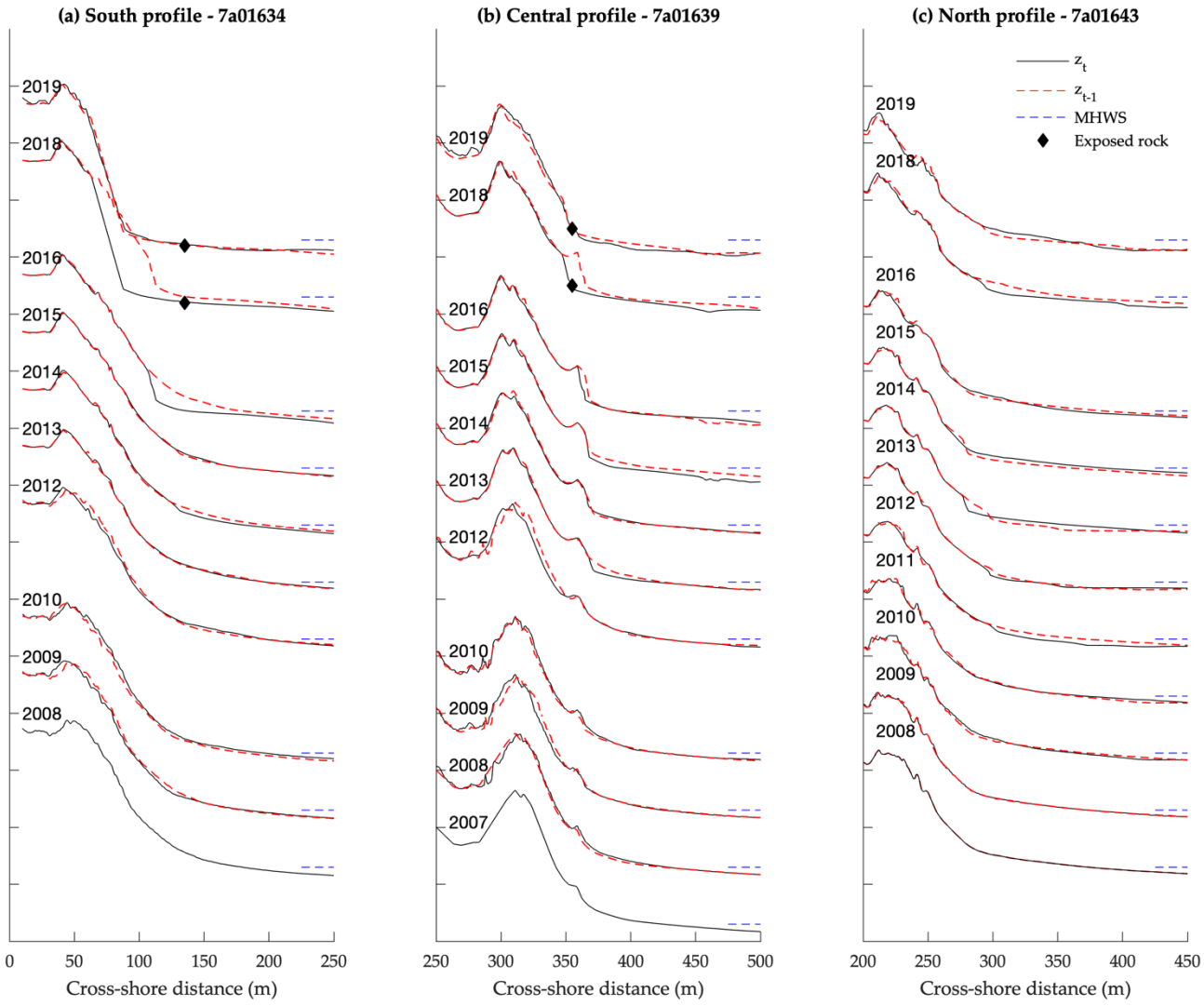

Figure 7. Topographic profile data from the North, Central and South profiles of Crantock Beach. The profiles have been vertically offset by 10 m to bring out the annual morphological changes (tick marks on the y-axis are every 10 m). The exposed bedrock on the profiles observed in 2018 and 2019 have been identified based on the feature codes provided in the survey data.

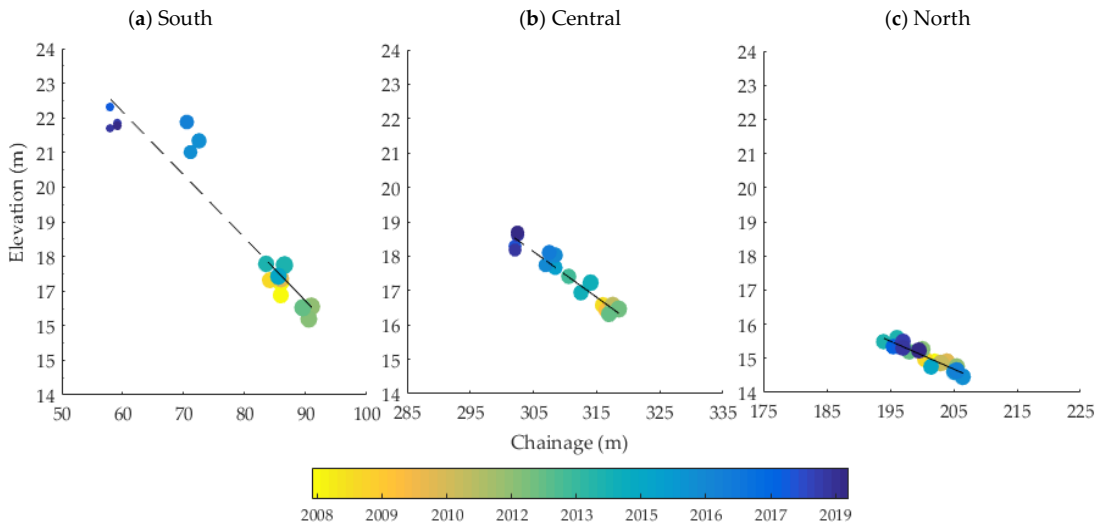

Figure 8. Change in the horizontal and vertical position of the centroid of the dune through time for (**a**) southern-most profile (7a01634), (**b**) central profile (7a01639), and (**c**) northern-most profile (7a01643). The size of the markers is relative to the percentage volume lost between each time step, exaggerated to the power of 3 for visual effect.

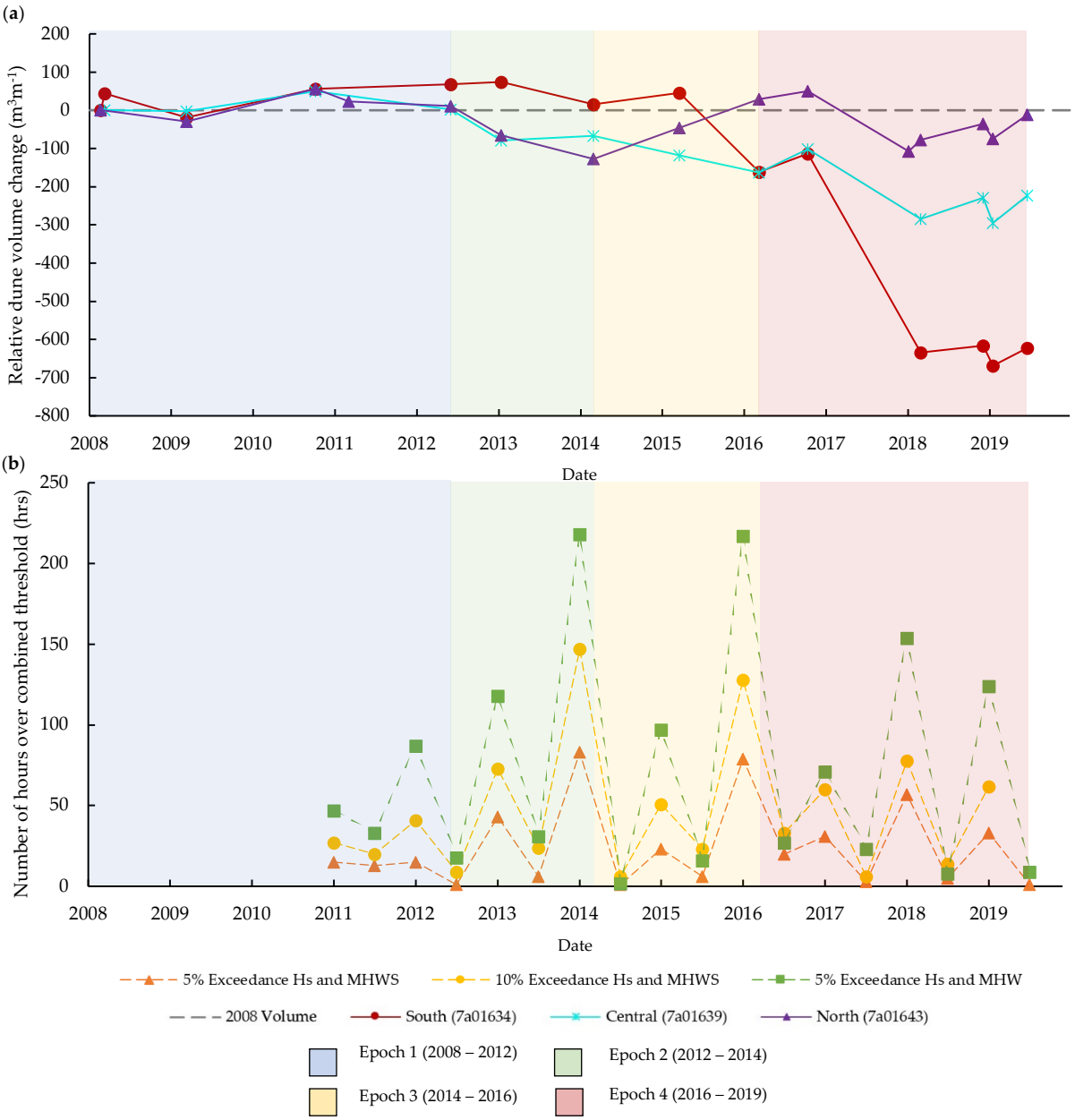

Figure 9. (**a**) Dune volume time series from the south, central and north profiles at Crantock beach against (**b**) number of hours per summer (April to October) and winter season (November to March) where significant wave heights (H_s) and water level (WL_{OD}) are sufficient to activate the dune face. Three threshold scenarios are defined here: 1) 5% exceedance H_s and MHWS; 2) 10% exceedance H_s and MHWS; and 3) 5% exceedance H_s and MHW.

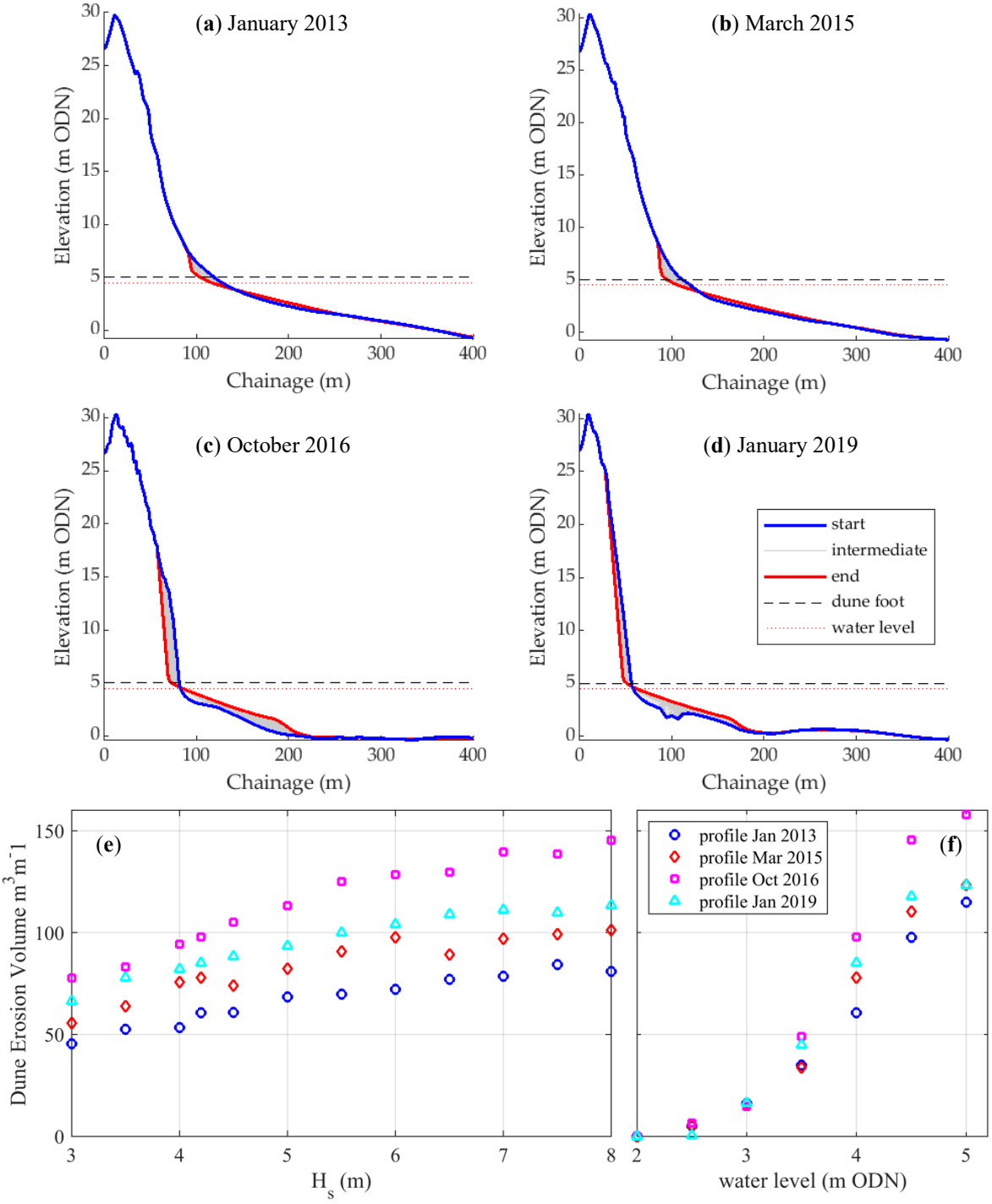

Figure 10. Model results from a sensitivity analysis conducted in XBeach. Results show the dune erosion response (**e and f**) under varying wave height (**e**, with water level = 4 m ODN) and water level (**f**, with H_s = 4.2 m) from 4 different initial profiles: (**a**) January 2013; (**b**) March 2015; (**c**) October 2016; and (**d**) January 2019. Post-storm profiles in **a-d** show the outcome from model runs with 1% exceedance H_s (4.2 m) and water level just below dune toe elevation (4.5 m ODN).